ACS Macro Letters

Letter

pubs.acs.org/macroletters

Combined Dependence of Nanoconfined T_g on Interfacial Energy and Softness of Confinement

Ryan J. Lang,[†] Weston L. Merling,[†] and David S. Simmons*

Department of Polymer Engineering, The University of Akron, 250 South Forge Street, Akron, Ohio 44325-0301, United States

Supporting Information

ABSTRACT: We employ molecular dynamics simulations of nanolayered polymers to systematically quantify the dependence of T_g nanoconfinement effects on interfacial energy and the "softness" of confinement. Results indicate that nanoconfined T_g depends linearly on interfacial adhesion energy, with a slope that scales exponentially with the ratio of the bulk Debye−Waller factors $\langle u^2 \rangle$ of the confined and confining materials. These trends, together with a convergence at low interfacial adhesion energy to the T_g of an equivalent freestanding film, are captured in a single functional form, with only three parameters explicitly referring to the confined state. The observed dependence on $\langle u^2 \rangle$ indicates that softness of nanoconfinement should be defined in terms of the relative high frequency shear moduli, rather than low frequency moduli or relaxation times, of the confined and confining materials.

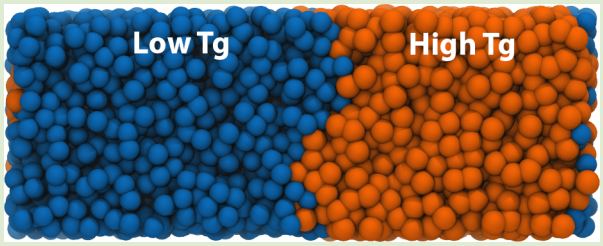

Confinement to nanoscale dimensions can profoundly alter the dynamic and mechanical properties of glass-forming liquids.[1−6] For example, the glass transition temperature T_g of a polystyrene nanofilm supported on silica is reduced by as much as 50 K from bulk, with associated alterations in mechanical[7] and transport[8] properties. Moreover, the magnitude and even direction of these shifts depend on system details: materials confined by rigid surfaces exhibit a crossover from T_g suppression to enhancement with increasing interfacial energy;[9,10] confinement by soft materials and free surfaces generally yields a reduction in T_g.[11−14] However, the exact meaning of the "softness" of confinement in terms of relative relaxation times or moduli is presently unclear. Given that T_g can exhibit shifts from 50 K suppression to 50 K enhancement with shifts in these properties, establishing a clear understanding of the dependence of nanoconfined T_g on interfacial energy and "softness" of confinement remains a key challenge in the understanding of nanoconfined systems.

In addition to materials with nanoscale dimensions, T_g nanoconfinement effects can impact bulk materials possessing internal nanostructure, including block copolymers,[15−23] bilayers,[19,24] multinanolayered polymers,[25,26] polymer/polymer nanocomposites,[11] polymer/inorganic nanocomposites,[27,28] stacked nanofilms,[29] and dilute blends.[30] These systems offer an excellent platform for study of nanoconfinement techniques due to their amenability to bulk characterization methods, rather than specialized metrologies designed for nanoscale materials. Furthermore, given the large number of systems exhibiting internal nanoconfinement, an understanding of nanoconfinement effects applicable to these systems would be of particular value in the rational control of advanced material properties. However, until recently, a majority of studies on polymer T_g nanoconfinement effects have investigated systems in which nanoconfinement is driven by overall nanoscale system dimensions. Accordingly, here we employ simulations of nanolayered polymers in order to study the combined dependence of confined T_g on interfacial energy and the softness of confinement. Results identify a clear quantitative measure of relative softness of confinement and lead to a single functional form capturing the effect of both of these variables.

Simulations consist of two explicitly modeled layers of a nanolayered polymer, with periodic boundaries imposed in all directions to reflect an infinitely nanolayered geometry. These simulations are also compared to freestanding film and bulk melt simulations described previously.[31] Simulations employ an attractive linear bead−spring polymer (described at length in the SI), based on the model of Kremer and Grest,[32] that has been used extensively to study polymer glass formation.[27,33−35] Unentangled polymers are modeled as 20-bead chains, with nonbonded beads of species i and j interacting via a 12−6 Lennard-Jones (LJ)[36] potential $E^{ij}_{LJ} = 4\varepsilon_{ij}[(\sigma/r)^{12} - (\sigma/r)^6]$. E^{ij}_{LJ} is truncated at a distance of 2.5σ, unless otherwise specified.[37] Bonded monomers interact via the finitely extensible nonlinear elastic (FENE)[36] potential.

In order to probe the role of relative layer "softness" and T_g, we simulate layered films in which the two polymers' pure-state T_gs differ by a factor of α. This is accomplished by taking advantage of the dimensionless nature of LJ units: the dimensionless LJ temperature T is defined with respect to real temperature T^* as $T = kT^*/\varepsilon$, and the LJ unit of time $\tau \sim (\varepsilon/m)^{1/2}$, where m is bead mass. These definitions rigorously imply that if two simulated materials are identical except that all interaction energy scales and masses in the second are

Received: June 18, 2014
Accepted: July 11, 2014
Published: July 23, 2014

   dx.doi.org/10.1021/mz500361v | ACS Macro Lett. 2014, 3, 758−762

multiplied by a factor α relative to the first, all thermodynamic and dynamic properties in the second at a temperature αT will be equal to those at a temperature T in the first. Accordingly, for the first polymer we employ energy and mass parameters from the standard Kremer-Grest model, while for the second polymer these parameters are multiplied by a factor of α while holding all other features of the model unchanged. Consequently, the pure-state properties of the two polymers are related via the above temperature rescaling, and the bulk T_g of the polymer 2 is α times the bulk T_g of polymer 1.

Polymer domains of 100 chains each are initially generated in a layered morphology and maintained in this geometry by fixing the box dimensions in the plane of the layers. Simulations are gradually quenched from high temperature at pressure $P = 0$ and then annealed at fixed T in the NPT ensemble, with a Nose-Hoover barostat coupled only to the component of pressure normal to the interface in order to avoid contamination by the interfacial tension. Data is then collected in NVT ensemble simulations continued from these equilibrations. This procedure yields layers of thickness $13-14\sigma$ near T_g (corresponding to a thickness of roughly 6.5−14 nm in real units[21,32,38]), with thickness increasing by about 1σ from T_g to $2T_g$ in accordance with the polymer's equation of state. To ensure good equilibration, data for a given layer at a given T are only employed if the layer's mean structural relaxation time τ_α (defined below) is at most 1% of the equilibration time. Error bars throughout this paper are standard deviations determined from four independent simulations of each system.

Polymer segmental relaxation is quantified via the self-part of the intermediate scattering function, $F_s(k,t)$, computed at a wavenumber $k = 7.07$, comparable to the first peak in the structure factor. τ_α is defined as the time at which $F_s(k,t)$ decays by 80%, employing a Kohlrausch−Williams−Watts stretched exponential fit[39,40] for data smoothing and interpolation. T_g is defined as the T at which $\tau_\alpha \rightarrow 10^3\tau$, the time scale beyond which these simulations begin to fall out of equilibrium.

In order to quantify the dependence of T_g/T_g^{bulk} on interfacial energy, we perform a series of simulations in which $\alpha = 1.5$ and the cross-interaction energy scale ε_{12} is varied from $0.3\varepsilon_{11}$ to $1.2\varepsilon_{11}$. The upper value of ε_{12} yielding an immiscible system is dictated at a mean field level by the requirement that the Flory χ parameter, which is proportional to the quantity $\Delta\varepsilon \equiv \varepsilon_{11} + \varepsilon_{22} - 2\varepsilon_{12}$, remain positive; the maximum ε_{12} is accordingly chosen such that $\Delta\varepsilon = 0.1$. We refer to the unmodified polymer as the low-T_g polymer (LTgP) and the modified polymer as the high-T_g polymer (HTgP). Finally, a system in which the cross-interaction is purely repulsive is also modeled by employing a cutoff distance of $2^{1/6}\sigma$ for LJ interactions between the HTgP and LTgP only, and with $\varepsilon_{12} = 1$.

Prior work suggests that nanoconfined T_g increases with increasing strength of polymer−substrate interaction energy[9,10] and that strong adhesion of polymer segments to an interface can enhance nanoconfined T_g. Within our model, the strength of the interfacial attractive interaction is proportional to the per-interaction attractive energy scale E_i, equal to ε_{12} in systems with attractive interactions between the two polymers or 0 in the system with fully repulsive cross interactions. Moreover, within a mean field model, E_i is expected to be proportional to the work of adhesion W_{12} required to separate two layers to an infinite distance, given by $W_{12} = [G_1^F + G_2^F + G_1^{ML}]/2A$, where G is the free energy, superscript "F" denotes the freestanding film state, superscript "ML" denotes a multilayer film comprised of freestanding films of species 1 and 2 brought into contact, and A is interfacial area. We emphasize that, in contrast to the interfacial energy γ_{12} that is defined with respect to a bulk reference state, W_{12} and E_i increase with increasing thermodynamic favorability of the interface. Specifically, $W_{12} = \gamma_1 + \gamma_2 + \gamma_{12}$, where γ_k is the surface energy of a freestanding film of component k, defined as the free energy per area required to create a surface within a pure sample of species k.[41] In order to validate the approximation that $E_i \propto W_{12}$, we compute W_{12} and γ_{12} as a function of E_i based on the pressure tensor in our simulations via the equation[42]

$$\gamma_{12} = \frac{L_z}{2}\left\langle P_{zz} - \frac{1}{2}(P_{xx} + P_{yy})\right\rangle \quad (1)$$

where L_z is the length of the box in the direction normal to the interface. As shown by Figure 1, this proportionality holds to within uncertainty over the range of ε_{12} considered here, and we therefore employ E_i as a noise-free and temperature-insensitive measure of work or energy of adhesion.

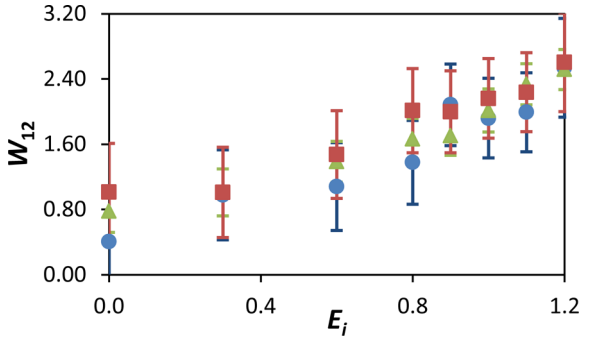

Figure 1. Work of adhesion versus per-interaction interfacial adhesion energy at $T = 0.72$ (green triangle), 0.66 (red square), and 0.60 (blue circle).

As shown by Figure 2, T_g/T_g^{bulk} for both the HTgP and LTgP in these systems exhibits a linear dependence on E_i. This result for the LTgP is consistent with experimental results for polystyrene and poly(methyl methacrylate) on silica substrates

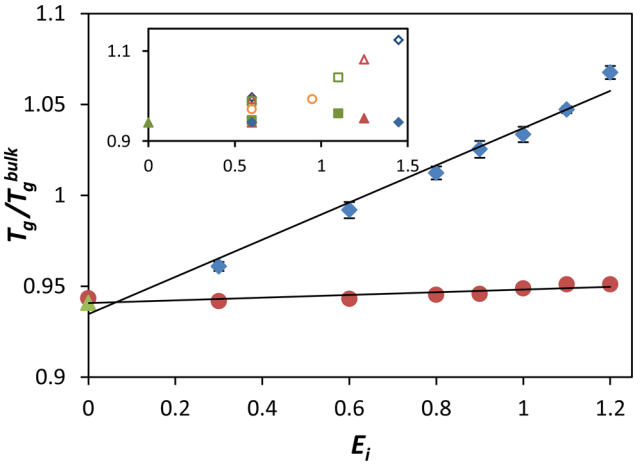

Figure 2. $T_g/T_{g,bulk}$ vs E_i for the LTgP (blue diamond) and HTgP (red circle) for a simulation in which $\alpha = 1.5$ and for a freestanding film (green triangle). Solid lines are linear fits. Inset shows the same plot of HTgP (filled symbols) and LTgP (open symbols) with $\alpha = 1$ (orange circle), 1.3 (green square), 1.6 (red triangle), and 2 (blue diamond).

dx.doi.org/10.1021/mz500361v | ACS Macro Lett. 2014, 3, 758−762

that were surface-modified to explore a range of interfacial energies.[10] As in that case, the LTgP also exhibits a crossover from T_g suppression to T_g enhancement with increasing interfacial adhesion energy. In contrast, T_g of the HTgP is suppressed for all interfacial energies. While the interfacial energy dependence of T_g under soft confinement has not been previously studied, such systems have generally been observed to exhibit T_g suppression,[11−13,19,20] consistent with these results.

Notably, T_g/T_g^{bulk} of the HTgP and LTgP become quantitatively indistinguishable at $E_i = 0$ from that of a corresponding freestanding film. At least at the level of T_g, there is apparently no difference between freestanding, hard, and soft confinement for a completely nonattractive interface. We attribute this outcome to the presence of a nearly complete interfacial density depletion at $E_i = 0$ (shown in Figure 3),

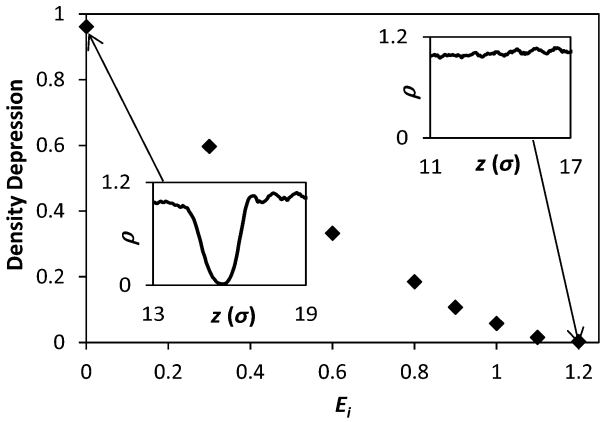

Figure 3. Magnitude of density depletion at the interface as a function of E_i at $T = 0.65$. Insets depict number density ρ near an interface at this T for the interfacial energies indicated. The ρ depression quantified in the main figure corresponds to the depth of the well, visible in the left inset.

where the density depletion is defined as the difference between the mean density averaged across the two layers and the density at the minimum. The presence of this strong minimum at low E_i implies that the layers in that case behave essentially as freestanding films in weak contact.

The combination of a linear dependence of T_g/T_g^{bulk} on E_i with convergence to the freestanding film result at $E_i = 0$ suggests that, to leading order, T_g/T_g^{bulk} obeys the form

$$\frac{T_g}{T_g^{bulk}} = \frac{T_g^{fs}}{T_g^{bulk}} + CE_i \qquad (2)$$

where T_g^{fs} is the T_g of a corresponding freestanding film. C is a constant that does not depend on interfacial energy but evidently depends on the "softness" of confinement, given that for this data $C = 0.10$ for the layer under "hard" confinement and 0.01 for the layer under "soft" confinement. As indicated in the introduction, it has been unclear how "softness" of confinement should be defined. We begin by testing the proposition that it depends upon the relative time scales of slow relaxation processes in the confined and confining materials. A simple measure of softness of confinement defined on this basis for a given layer is provided by the ratio $T_{g,bulk}^{confining}/T_{g,bulk}^{confined}$ of the bulk T_g of the polymer comprising the other layer to the bulk T_g of the polymer comprising that layer. For example, $T_{g,bulk}^{confining}/T_{g,bulk}^{confined}$ equals 1.5 and 1/1.5 for the LTgP and HTgP, respectively, in the study described above.

In order to quantify the dependence of C on $T_{g,bulk}^{confining}/T_{g,bulk}^{confined}$, we perform a series of simulations in which α is varied from 1 to 2, and for each value of α we perform a simulation for which $\varepsilon_{12} = 0.6$ and one for which ε_{12} is selected such that $\Delta\varepsilon = 0.1$. As shown in the inset of Figure 2, the dependence of $T_g/T_{g,bulk}$ on E_i remains approximately linear over this range of α, and a fit of eq 2 to $T_g/T_{g,bulk}$ at each α thus yields C for that layer. As shown by Figure 4a, C versus $T_{g,bulk}^{confining}/T_{g,bulk}^{confined}$ exhibits

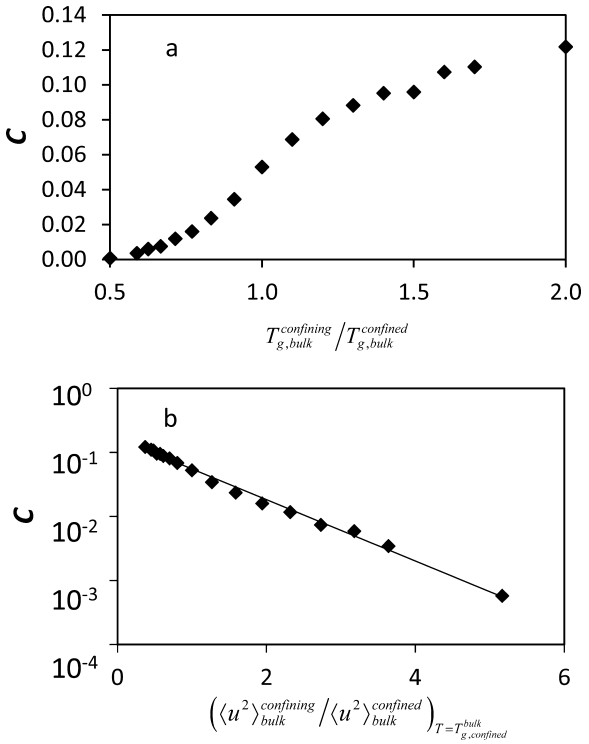

Figure 4. (a) Strength C of the dependence of $T_g/T_{g,bulk}$ on E_i as a function of $T_{g,bulk}^{confining}/T_{g,bulk}^{confined}$. (b) The same data plotted on a log scale vs $\langle u^2\rangle_{bulk}^{confining}/\langle u^2\rangle_{bulk}^{confined}$. The solid line is an exponential fit to the data. Error bars lie within the points.

an inflection point near $T_{g,bulk}^{confining}/T_{g,bulk}^{confined} = 1$. For $T_{g,bulk}^{confining}/T_{g,bulk}^{confined} < 1$, C depends strongly on $T_{g,bulk}^{confining}/T_{g,bulk}^{confined}$; for $T_{g,bulk}^{confining}/T_{g,bulk}^{confined} > 1$, its dependence is weaker and more linear. Notably, these two regimes correspond to conditions under which the confining material is liquid and glassy, respectively, at the T_g of the confined material. Given the qualitative differences between these two regimes, it seems unlikely that C is fundamentally controlled by the relative time scales of slow relaxation processes in the two layers, as measured by $T_{g,bulk}^{confining}/T_{g,bulk}^{confined}$.

Alternatively, the confined T_g may be sensitive to the relative strength of fast dynamics in the two films. This possibility would be consistent with the expectation that confined T_g is impacted by the "hardness", or modulus, of the confining surface. The Debye−Waller factor $\langle u^2\rangle$, which is a measure of segmental "rattle-space" on a picosecond time scale, provides a measure of fast dynamics with strong connections to diffusion, reaction, and relaxation rates in glass-forming liquids.[43,44] Moreover, $\langle u^2\rangle$ is more closely linked to layer "hardness" than is T_g: previous studies have, on the basis of a Maxwell model, argued for a rough proportionality between the high frequency

dx.doi.org/10.1021/mz500361v | ACS Macro Lett. 2014, 3, 758−762

shear modulus and the quantity $k_BT/\langle u^2\rangle$.[43,45−47] A dependence of T_g on the ratio of $\langle u^2\rangle$ in the confining and confined materials would therefore be qualitatively consistent with the observed dependence on relative stiffness of these materials. Accordingly, in Figure 4b we replot C versus the ratio $\langle u^2\rangle_{bulk}^{confining}/\langle u^2\rangle_{bulk}^{confined}$ for each layer, where, in accordance with prior studies,[43,48,49] we define $\langle u^2\rangle$ as the mean square displacement at a time of 1τ (corresponding to approximately 1 to 10 ps in real units). We focus on $\langle u^2\rangle$ as measured in the bulk to avoid relying on experimentally difficult thin film $\langle u^2\rangle$ values, and we use its value at the bulk T_g of the confined material as a convenient convention. As shown by Figure 4b, C exhibits an exponential dependence on $\langle u^2\rangle_{bulk}^{confining}/\langle u^2\rangle_{bulk}^{confined}$:

$$C = A\ \exp\left(-B\frac{\langle u^2\rangle_{bulk}^{confining}}{\langle u^2\rangle_{bulk}^{confined}}\right) \tag{3}$$

where for this system $A = 0.17$ and $B = 1.1$ with coefficient of determination $R^2 = 0.99$. This simple dependence of C on $\langle u^2\rangle_{bulk}^{confining}/\langle u^2\rangle_{bulk}^{confined}$ suggests that softness of confinement should be defined based upon the relative Debye−Waller factors or, alternatively, high frequency shear moduli of the confined and confining materials, rather than upon their relative relaxation times or lower-frequency moduli.

Combination of eqs 2 and 3 suggests a master equation describing the effects of interfacial adhesion energy and the ratio of $\langle u^2\rangle$ between the two layers on confined T_g:

$$\frac{T_g}{T_g^{bulk}} = \frac{T_g^{fs}}{T_g^{bulk}} + AE_i\ \exp\left(-B\frac{\langle u^2\rangle_{bulk}^{confining}}{\langle u^2\rangle_{bulk}^{confined}}\right)\Bigg|_{T_{g,bulk}^{confined}} \tag{4}$$

where A and B do not depend to leading order on E_i or $\langle u^2\rangle$ but may be a function of the specific confined material and of layer thickness. Equation 4 contains only three quantities specific to the confined state: T_g^{fs}/T_g^{bulk} quantifies the T_g suppression in an equivalent freestanding film; A quantifies the dependence of T_g/T_g^{bulk} on E_i for a material sandwiched between completely hard confining surfaces; and B quantifies how rapidly this dependence weakens as the relative stiffness of the confining material is reduced. Since other quantities are defined in the bulk state, eq 4 enables prediction of nanoconfined T_g based upon characterization of only three nanoconfined states for a given material at a given thickness.

How can the dependences captured by eq 4 be physically rationalized? First, a simple activation model of relaxation leads to a linear dependence of T_g on E_i, since T_g is proportional to the activation energy E_a of segmental relaxation, and E_a near the interface can be expected to scale linearly in E_i. Alternatively, Shi, Jiang, and co-workers have proposed[50,51] a Lindemann theory of glass formation under nanoconfinement that, in the limit of low works of adhesion, predicts a linear dependence of T_g on E_i (see Supporting Information). However, neither of these models apparently yield an exponential dependence on $\langle u^2\rangle_{bulk}^{confining}/\langle u^2\rangle_{bulk}^{confined}$. Qualitatively, this dependence yields reasonable limiting behavior: C goes to zero for perfectly soft confinement ($\langle u^2\rangle_{bulk}^{confining}/\langle u^2\rangle_{bulk}^{confined} \to \infty$) and to a fixed finite value for perfectly hard confinement ($\langle u^2\rangle_{bulk}^{confining}/\langle u^2\rangle_{bulk}^{confined} \to 0$). We suggest that further insight into this dependence will require characterization of interfacial gradients in $\langle u^2\rangle$ and τ_α. A future paper will examine these quantities for the nanolayered systems considered here.

In summary, on the basis of molecular dynamics simulations of nanolayered films, we propose a master equation describing the combined impacts of interfacial adhesion energy and softness of confinement on nanoconfined T_g. The data on which this model is based is obtained for relatively low molecular weight polymers; we therefore expect this form to apply over the broad range of molecular weights for which no appreciable molecular weight dependence of nanoconfined T_g is observed in freestanding films (less than approximately 350 kg/mol for polystyrene, for example).[52] This form specifically identifies the ratio of Debye−Waller factors of the confined and confining materials, as measured in the bulk, as a key "softness" parameter controlling confinement effects on T_g. In contrast, the materials' relative T_g and, therefore, their relative structural relaxation time, is somewhat less informative. This may explain why polystyrene supported on liquid glycerol exhibits T_g suppression substantially weaker than freestanding PS films,[53] since glycerol relaxes quickly but has a relatively low $\langle u^2\rangle$.[54,55] Observed qualitative agreement between results of these simulations and experimental results in other geometries suggests that the proposed functional form may also describe systems such as supported films, block copolymers, and colloids. This potential master form could therefore provide a valuable new tool in the design of nanostructured materials. Finally, these results emphasize the potential of bulk internally nanostructured systems to provide a valuable setting for the study of nanoconfinement effects on the glass transition.

■ ASSOCIATED CONTENT

Supporting Information

Additional information on simulation methodology and analysis, and linearization of Lindemann theory of nanoconfined glass formation of Shi, Jiang, and co-workers in the limit of low interfacial energy. This material is available free of charge via the Internet at http://pubs.acs.org.

■ AUTHOR INFORMATION

Corresponding Author

*E-mail: dsimmon@uakron.edu.

Author Contributions

†These authors contributed equally (R.J.L. and W.L.M.).

Notes

The authors declare no competing financial interest.

■ ACKNOWLEDGMENTS

This material is based on work supported by the National Science Foundation under Grant No. DMR1310433. This work used the Extreme Science and Engineering Discovery Environment (XSEDE), which is supported by National Science Grant No. OCI-1053575 (XSEDE Grant Nos. DMR120019 and DMR130011). The authors thank Bryan Vogt and Jack Douglas for editorial advice and helpful discussions.

■ REFERENCES

(1) Keddie, J. L.; Jones, R. A. L.; Cory, R. A. *Europhys. Lett.* **1994**, *27*, 59−64.

(2) Forrest, J.; Dalnoki-Veress, K.; Dutcher, J. *Phys. Rev. E* **1997**, *56*, 5705−5716.

(3) Jackson, C. L.; McKenna, G. B. *J. Non-Cryst. Solids* **1991**, *131*−*133* (Part 1), 221−224.

(4) Richert, R. In *Structural Glasses and Supercooled Liquids*; Wolynes, P. G., Lubchenko, V., Eds.; John Wiley & Sons, Inc.: New York, 2012; pp 1−30.

(5) McKenna, G. B. *Eur. Phys. J.: Spec. Top.* **2010**, *189*, 285−302.
(6) Ediger, M. D.; Forrest, J. A. *Macromolecules* **2014**, *47*, 471−478.
(7) Torres, J. M.; Stafford, C. M.; Vogt, B. D. *ACS Nano* **2009**, *3*, 2677−2685.
(8) Zheng, X.; Rafailovich, M. H.; Sokolov, J.; Strzhemechny, Y.; Schwarz, S. A.; Sauer, B. B.; Rubinstein, M. *Phys. Rev. Lett.* **1997**, *79*, 241−244.
(9) Torres, J. A.; Nealey, P. F.; de Pablo, J. J. *Phys. Rev. Lett.* **2000**, *85*, 3221−3224.
(10) Fryer, D. S.; Peters, R. D.; Kim, E. J.; Tomaszewski, J. E.; Nealey, P. F. *Macromolecules* **2001**, *34*, 5627.
(11) Rharbi, Y. *Phys. Rev. E* **2008**, *77*, 031806.
(12) He, F.; Wang, L. M.; Richert, R. *Phys. Rev. B* **2005**, *71*, 144205.1−144205.10.
(13) Zhang, C.; Guo, Y.; Priestley, R. D. *Macromolecules* **2011**, *44*, 4001−4006.
(14) Zhang, C.; Priestley, R. D. *Soft Matter* **2013**, *9*, 7076−7085.
(15) Cooper, S. L.; Tobolsky, A. V. *J. Appl. Polym. Sci.* **1966**, *10*, 1837−1844.
(16) Bares, J. *Macromolecules* **1975**, *8*, 244−246.
(17) Krause, S.; Iskandar, M.; Iqbal, M. *Macromolecules* **1982**, *15*, 105−111.
(18) Rosati, D.; Perrin, M.; Navard, P.; Harabagiu, V.; Pinteala, M.; Simionescu, B. C. *Macromolecules* **1998**, *31*, 4301−4308.
(19) Roth, C. B.; Torkelson, J. M. *Macromolecules* **2007**, *40*, 3328−3336.
(20) Robertson, C. G.; Hogan, T. E.; Rackaitis, M.; Puskas, J. E.; Wang, X. *J. Chem. Phys.* **2010**, *132*, 104904.
(21) Slimani, M. Z.; Moreno, A. J.; Colmenero, J. *Macromolecules* **2011**, *44*, 6952−6961.
(22) Slimani, M. Z.; Moreno, A. J.; Colmenero, J. *Macromolecules* **2012**, *45*, 8841−8852.
(23) Slimani, M. Z.; Moreno, A. J.; Rossi, G.; Colmenero, J. *Macromolecules* **2013**, *46*, 5066−5079.
(24) Rauscher, P. M.; Pye, J. E.; Baglay, R. R.; Roth, C. B. *Macromolecules* **2013**, *46*, 9806−9817.
(25) Liu, R. Y. F.; Bernal-Lara, T. E.; Hiltner, A.; Baer, E. *Macromolecules* **2005**, *38*, 4819−4827.
(26) Arabeche, K.; Delbreilh, L.; Saiter, J.-M.; Michler, G. H.; Adhikari, R.; Baer, E. *Polymer* **2014**, *55*, 1546−1551.
(27) Starr, F. W.; Douglas, J. F. *Phys. Rev. Lett.* **2011**, *106*, 115702.
(28) Starr, F. W.; Douglas, J. F. *arXiv Cond. Mat.* **2009**, arXiv:0906.5275.
(29) Koh, Y. P.; McKenna, G. B.; Simon, S. L. *J. Polym. Sci., Part B: Polym. Phys.* **2006**, *44*, 3518−3527.
(30) Evans, C. M.; Sandoval, R. W.; Torkelson, J. M. *Macromolecules* **2011**, *44*, 6645−6648.
(31) Lang, R. J.; Simmons, D. S. *Macromolecules* **2013**, *46*, 9818−9825.
(32) Kremer, K.; Grest, G. S. *J. Chem. Phys.* **1990**, *92*, 5057−5086.
(33) Varnik, F.; Baschnagel, J.; Binder, K. *Phys. Rev. E* **2002**, *65*, 021507.
(34) Buchholz, J.; Paul, W.; Varnik, F.; Binder, K. *J. Chem. Phys.* **2002**, *117*, 7364−7372.
(35) Hanakata, P. Z.; Douglas, J. F.; Starr, F. W. *J. Chem. Phys.* **2012**, *137*, 244901.
(36) Grest, G. S.; Kremer, K. *Phys. Rev. A* **1986**, *33*, 3628−3631.
(37) Starr, F. W.; Schroder, T. B.; Glotzer, S. C. *Macromolecules* **2002**, *35*, 4481−4492.
(38) Baschnagel, J.; Varnik, F. *J. Phys.: Condens. Matter* **2005**, *17*, R851−R953.
(39) Kohlrausch, F. *Ann. Phys. (Berlin, Ger.)* **1863**, *119*, 352.
(40) Williams, G.; Watts, D. C. *Trans Faraday Soc.* **1970**, *66*, 80−85.
(41) Israelachvili, J. *Intermolecular and Surface Forces*, 2nd ed.; Academic Press: London, 1992.
(42) Harris, J. G. *J. Phys. Chem.* **1992**, *96*, 5077−5086.
(43) Simmons, D. S.; Douglas, J. F. *Soft Matter* **2011**, *7*, 11010−11020.
(44) Cicerone, M. T.; Douglas, J. F. *Soft Matter* **2012**, *8*, 2983−2991.
(45) Van Zanten, J. H.; Rufener, K. P. *Phys. Rev. E* **2000**, *62*, 5389−5396.
(46) Dudowicz, J.; Freed, K. F.; Douglas, J. F. *Advances in Chemical Physics*; Wiley: New York, 2008; Vol. *137*, pp 125−222.
(47) Puosi, F.; Leporini, D. *arXiv:1108.4629* **2011**.
(48) Larini, L.; Ottochian, A.; De Michele, C.; Leporini, D. *Nat. Phys.* **2008**, *4*, 42−45.
(49) Simmons, D. S.; Cicerone, M. T.; Zhong, Q.; Tyagi, M.; Douglas, J. F. *Soft Matter* **2012**, *8*, 11455−11461.
(50) Shi, F. G. *J. Mater. Res.* **1994**, *9*, 1307−1314.
(51) Jiang, Q.; Lang, X. Y. *Macromol. Rapid Commun.* **2004**, *25*, 825−828.
(52) Pye, J. E.; Roth, C. B. *Phys. Rev. Lett.* **2011**, *107*, 235701.
(53) Wang, J.; McKenna, G. B. *J. Polym. Sci., Part B: Polym. Phys.* **2013**, *51*, 1343−1349.
(54) Wuttke, J.; Petry, W.; Coddens, G.; Fujara, F. *Phys. Rev. E* **1995**, *52*, 4026−4034.
(55) Cicerone, M. T.; Soles, C. L. *Biophys. J.* **2004**, *86*, 3836−3845.